JMEPEG (2007) 16:418–431
DOI: 10.1007/s11665-007-9077-4
©ASM International
1059-9495/$19.00

Non-Steady-State Creep Behavior in Tube Gas Forming

Xin Wu

(Submitted February 1, 2007; in revised form March 27, 2007)

A steady-state creep equation is commonly used in the analysis of superplastic forming or other elevated temperature forming processes. However, in Hot Metal Gas Forming of tubes, the effective stress increases as tube diameter expands and wall thickness decreases, and a steady-state creep condition does not exist. Thus, non-steady-state creep behavior of materials becomes important. This paper presents some experimental results on transient creep behavior of a magnesium alloy, and provides an analysis on transient creep behavior and its application in tube forming mechanics. It is verified that non-steady-state creep plays important role in the gas tube forming at elevated temperatures.

Keywords automotive, mechanical testing, modeling processes, shaping

1. Introduction

In recent years, significant progress has been made in developing lightweight materials and automotive body structure manufacture techniques, in order to reduce energy consumption and environmental pollution, and to increase vehicle structural reliability and safety. Lighter weight structures are now to be made from light metals such as aluminum and magnesium alloys, and from various advanced high-strength steels (Ref 1). Common problems related to the application of these advanced materials include their relatively poor formability and high raw material cost. To overcome these two major barriers several thermally activated forming techniques have been developed, for example Quick Plastic Forming (QPS) (Ref 2), Hot Metal Gas Forming (HMGF) (Ref 3), and Hot Stamping (Ref 4).

The flow behavior and formability of metals under thermal activation are dependent not only on strain path during forming, but strain rate and temperature as well. Microstructural evolution during deformation at elevated temperatures further increases the complexity of the process. On the other hand, due to the high strain rate and temperature sensitivity of materials, it provides new means and opportunities for better control of metal flow and better product design. In order to take full advantage of thermal forming, it is of vital importance to understand material flow behavior at elevated temperatures.

In the traditional superplastic forming process that has been widely adopted in aerospace and aircraft component forming, the strain rate is usually in the order of 10^{-3} s^{-1}, so that the total creep deformation is mainly controlled by steady-state creep, while the primary creep has limited effect. However, at higher strain rate, say above 10^{-1} s^{-1}, which is often required for large-volume manufacturing such as that in automotive application, the forming cycle time is in a few seconds up to 1 min, within which a steady-state creep condition may not be reached, and the contribution of the primary creep to the total deformation can not be ignored.

The current author was previously involved in the initial development of HMGF process (Ref 5, 6). In this process a tubular or hollowed component is bulged under a gas pressure to against the ceramic die cavity wall. The workpiece is inductively preheaded inside the die through the embedded induction coil underneath the ceramic die surface, allowing rapid heating of the workpiece without heating up the die. The primary controlling parameters for the HMGF process are: the gas pressure profile $p(t)$, the temperature profile and distribution $T(X, t)$, and the end-feeding velocity profile $V(t)$ or force profile $F(t)$, where t is the forming time and X is the location of the workpiece. In tube HMGF, the hoop stress of the tube is not constant even though a constant gas pressure may be applied, due to a continuous increase in tube diameter and decrease in wall thickness. As a result, the material creep deformation is achieved not under a constant applied stress, but under a condition involving significant change of applied stress within a relatively short forming time. It was found that analysis based on a steady-state material equation obtained from tensile test often fail to correctly predict forming time. Among many uncertainties involved in hot deformation, the effect of primary creep on deformation rate can be one of possible root causes that deserve a careful investigation.

In this paper, the main objective is to provide an early assessment on the contribution of transient creep to the total deformation in HMGF, and the factors affecting the transient creep. For this purpose, a review of classical theory of primary creep will be reviewed first. Then a simple kinetic model is used to analyze the transient stress development. With these preparations, the transient creep behavior of an Mg AZ31 tube material is analyzed and the transient kinetics is experimentally investigated. Finally, the HMGF mechanics with and without consideration of transient creep behavior are analyzed and compared.

This article was presented at Materials Science & Technology 2006, Innovations in Metal Forming symposium held in Cincinnati, OH, October 15-19, 2006.

Xin Wu, Department of Mechanical Engineering and Institute for Materials Research, Wayne State University, Detroit, MI 48202. Contact e-mail: xwu@eng.wayne.edu.

2. Background

2.1 Steady-State Creep

At elevated temperature ($T > 0.4T_m$, where T_m is the melting point), plastic deformation of polycrystalline materials may be controlled by various mechanisms that may be divided into two main categories of dislocation creep and diffusional creep. Extensive research has been conducted on the atomistic creep equations based on different rate-controlling processes. Ashby and Verrall (Ref 7) summarized various deformation mechanisms and proposed a deformation mechanism map. As they pointed out, the deformation behavior of solids is determined by the kinetics of the processes occurring on the atomic scale. The creep rate can be represented by a general rate equation,

$$\dot{\varepsilon} = A\frac{DGb}{kT}\left(\frac{b}{d}\right)^{p}\left(\frac{\sigma - \sigma_0}{G}\right)^{N}, \qquad \text{(Eq 2.1)}$$

where k—The Boltzmann's constant; σ_o—Threshold stress for creep; b—Burger's vector; D—Diffusivity through various paths indicated by a subscript: gb—grain boundary, p—dislocation pipe, L—lattice, sol—solid solution. The temperature dependence of the diffusivity is given by $D = D_o\exp(-Q/RT)$, where Q is activation energy and R is the gas constant (= 8.31 J/K); G—the shear modulus and Young's modulus; d—Grain size, and p; N, p and A—the dimensionless material constants. N is the reciprocal of the strain rate sensitivity m ($m = 1/N$). Depending on the dominating deformation mechanisms under the regimes of applied stress, grain size, and temperature, the ranges of N and p values are different: At a high stress and strain rate material flow is controlled by plastic flow. At intermediate stresses, power law creep is the dominant mechanism, which gives N = 3-5 and $p = 0$. While at relative low stresses, either grain boundary diffusion or volume diffusion is the dominant mechanism. At relatively high stress, if grain size is large, there is no grain size dependence (or $p \approx 0$), but for a relatively small grain size there is an inverse dependence on d ($p \approx 2$) for volume diffusion and $p \approx 3$ for grain boundary diffusion.

A simplified form of Eq 2.1 was often used to describe the stress and temperature dependence, the only two state variables for a steady-state creep of an isotropic polycrystalline solid,

$$\dot{\varepsilon} = C\sigma^N = C_0\sigma^N \exp\left(-\frac{Q}{RT}\right) \qquad \text{(Eq 2.2)}$$

The parameters N, Q, and C_0 are constants within a given temperature-stress (or strain rate) range when deformation mechanisms do not change, and they can be experimentally determined from the tensile data set of (σ, ε, T).

2.2 Transient Creep

Upon changing of strain rate or applied stress the microstructure changes (e.g., rearranging dislocation network) that takes a transition period for the creep process to reach a new steady-state condition. For the increase of applied stress, the transient creep rate is faster than that predicted by steady-state creep, called normal transient, which has been studied and modeled by Dorn (Ref 8), Bird et al. (Ref 9), and Webster et al. (Ref 10). In this case the total strain was given by

$$\varepsilon = \varepsilon_p\{1 - \exp(-C\dot{\varepsilon}_{ss}t)\} + \dot{\varepsilon}_{ss}t. \qquad \text{(Eq 2.3)}$$

The strain rate, converted from their original primary strain expression, consists of two terms,

$$\dot{\varepsilon} = \dot{\varepsilon}_{pri} + \dot{\varepsilon}_{ss}. \qquad \text{(Eq 2.4)}$$

Much work on creep recovery has been done on structural response to the change of applied stress, for a creep strain rate in the order of 10^{-6} s^{-1}. For the case of unloading, when the initial strain rate is relatively high, a drop of applied stress will lead to a progressive lowering of the forward creep rate until, at a characteristic condition, no creep is detected, as reported in earlier work by Ahlquish and Nix (Ref 11) who observed negative creep upon increased stress drop until the remaining applied stress is lower than the internal stress σ_i. In another case when the initial strain rate is very low, the recovery-controlled creep might dominate, so that a small stress reduction would be followed by a stagnation period Δt when no change of specimen length is detected, and after that the forward creep resumes at a reduced rate. A detailed analysis and experimental evidence on the strain-transient process was reported by Henderson and McLean for a nickel-base superalloys (Ref 12).The strain transient following a stress change may simply be treated as the sum of the anelastic contraction and the reduced forward creep rate, as suggested by Lloyd and McElroy (Ref 13). For creep with large strain, a large body of literature is available on superplasticity and superplastic forming; however, due to a long forming time almost all the studies use a steady-state creep equation that is found satisfactory.

Transient creep was studied for various monolithic and composite material systems. Class II metal creep behavior of 2124 Aluminum alloy was reported by Li et al. (Ref 14), in which the creep rate in the transient region after a stress increase is faster than the new steady-state creep, and equiaxed subgrains are developed. On the other hand, Class I creep transient was reported for commercial AA5083 alloy (Ref 15, 16). For this class of metal the solute drag creep dominates deformation at fast strain rates and low temperature. The stress transients following strain-rate changes decay exponentially with strain, being contrast to those displayed by pure metals and Class II alloys. This "inverse" transient was modeled based on a graphical construction of experimental data.

The transient creep is generally associated with the internal stress development during load change. Orlova (Ref 17, 18) studied internal stress from strain-transient dip test in a Fe-3 wt.%Si alloy with a heterogeneous dislocation structure. The transient process is analyzed with a phenomenological model considering two components, as well as a dislocation kinetics model. Montemayoraldrete et al. (Ref 19) reported a sigmoidal transient creep behavior of a Cu-16 at.%Al alloy that is associated with the internal stress development. For composite systems the transient creep behavior can be more clearly explained from the internal stress development and stress transfer during a load change. For example, for Al-Al_2O_3 fiber composite (Ref 20), for an aluminum matrix composite (Ref 21), or for the composite with dilute and randomly oriented spheroidal inclusions (Ref 22).

The transient creep is also reported for Intermetallics. Hemker et al. (Ref 23) studied the transient behavior of Ni_3Al in which octahedral dislocation glide is the rate-controlling mechanism. In this study several experimental methods were used, including temperature change test, stress relaxation test, and deformation exhaustion/temperature drop tests.

The modeling of the transient creep may be based on an elasto-plastic constitutive behavior (Ref 24), or based on a two-phase composite model with different configurations such

as hard phase (Ref 25, 26), subgrains of variable volume fraction (Ref 27), particulate reinforcement (Ref 28), fiber reinforcement (Ref 29, 30). In all these studies it can be seen that the fundamental reason for transient creep behavior is the microstructural change and the internal stress transfer among constituents during dynamic change of applied stress (or strain rate).

2.3 Creep of Magnesium Alloys

The present study involves the use of magnesium AZ31; thus, some previous studies on magnesium creep deformation are briefly reviewed here. For wrought magnesium alloy with (h.c.p.) crystal structure it is well known that basal slip is the most important dislocation slip system. But the number of slip systems is limited for magnesium at room temperature. Other than basal slip, deformation twinning is an important deformation mechanism at room to intermediate temperatures (~673 K). With increasing temperature the contribution of the twinning to total deformation gradually decreases. Detailed deformation twinning was reported by several researchers (Ref 31-35). The twinning process not only accommodates a certain amount of shape change itself, but it also partially changes the crystallographic orientation and thus regenerates favorable basal slip system. At above 623 K, power law creep and diffusional creep take place, and which one is dominating depends on temperature, grain size, and applied stress or strain rate. Some creep studies for the power-exponent (N-value), activation (Q-value), and suggested mechanisms are listed in Table 1. With many more papers being published recently this table represents a snapshot in time. Note that the material data given in the last reference in the table are used in the computation in the present paper.

From the above studies it can be seen that with increasing temperature, more deformation processes operate and the mechanism becomes more complex. The reported creep parameters (activation energy, power-law stress exponent etc.) vary among different systems and conditions. In general, at intermediate temperature and low stress the deformation is controlled by viscous glide related to lattice diffusion (Class A creep), with $N \sim 3$, and at a high stress the $N \sim 7$, with the thermal activation energy about 140 kJ/mol corresponding to a lattice diffusion of Mg. At very high temperature $N \sim$ 4-5 with higher thermal activation energy, but it reduces with the applied stress. It must be noted that in many practical deformation process more than one deformation processes may operates, for example grain boundary diffusion and lattice diffusion may cooperate for a microstructure with a distributed grain size (as always), giving the apparent material parameters that often deviate from a pure theoretical creep equation.

3. Analysis of Transient Creep

For transient creep, now let us consider a strain rate-sensitive material that shows increased creep resistance at higher strain rate. We define a time-dependent creep resistance σ_R associated with material internal stress or microstructure. When a specimen is initially loaded from a stress-free state to a constant stress σ_a, σ_R will develop in response to the applied stress increase, and after certain time period a steady state will be reached at which $\sigma_R = \sigma_a$. This transient process exists whenever the applied stress changes. The time required for the resistance to catch up with the applied stress from one steady state to another depends on the kinetics of stress transition or microstructure change. With the first-order approximation we may assume that the rate of change in the internal creep resistance, $\dot{\sigma}_R$, is proportional to the difference between the applied stress and the current resistance stress σ_R, ($\sigma_a - \sigma_R$), which is the driving force for the stress transition, i.e.,

$$\dot{\sigma}_R = -k(\sigma_a - \sigma_R), \qquad \text{(Eq 3.1)}$$

where k is a temperature-dependent kinetic time constant for internal stress transition. By integration and with the use of initial condition $\sigma_R = 0$ at $t = 0$, the transient resistance development over time t in the primary creep can be expressed as

$$\sigma_R = \sigma_a\{1 - \exp(-kt)\}. \qquad \text{(Eq 3.2)}$$

Although mathematically the time required for σ_R to reach the applied stress σ_a would be $t = \infty$, only finite time is needed for real transition to complete. This is one drawback of this model but it is simple and convenient for current task. To get around the problem in the last stage of transition we may use a finite time $t_{0.05}$ for 5% residual at $\sigma_R = 0.95\sigma_a$,

$$t_{0.05} = -\ln(0.05)/k \approx 3.0/k \qquad \text{(Eq 3.3)}$$

For generality, we can treat the transient creep for stress transition between any two stress states from $\sigma_{a,1}$ to $\sigma_{a,2}$, so the resistance change rate $\dot{\sigma}_R$ is proportional to the difference

Table 1 A summary of previous study on creep of magnesium alloys

Author	Material	Temperature, K	Appl. stress, MPa or strain rate, s^{-1}	N	Q, kJ/mol	Suggested mechanisms/ creep laws
Northwood et al. (Ref 36)	Pure Mg	$T < 523$	10^{-4}-10^{-2}	...		Exponential law
		523-623		7		Power law
		673-773		2.2		
	Mg-Zn alloy	$T < 473$		7		Exponential law
		$T > 473$		5		Power law
Vagarali and Langdon (Ref 37)	Mg-0.8%Al	473 to 500-750	Low stress	3	140	Dislocation viscous glide (Class A)
			High stress	6	140	Dislocation climb (break away from solute atmospheres)
		>500-750		4	230	
Regev et al. (Ref 38)	AZ91D (Coarse-grain)	393-453	40-115		220 to 94 (decrease with T)	
Wu and Liu (Ref 39)	AZ31	623-773	10^{-4}-10^{-2}	2.6	145	Lattice diffusion of magnesium

$(\sigma_{a,2} - \sigma_{a,1})$. By integration with the initial condition of $\sigma_R = \sigma_{a,1}$ at $t = 0$, we get the stress evolution as a function of time t,

$$\sigma_R(t) = \sigma_{a,2} - (\sigma_{a,2} - \sigma_{a,1}) \exp(-kt), \quad \text{(Eq 3.4)}$$

where t is from the moment when the applied stress changes from $\sigma_{a,1}$ to $\sigma_{a,2}$. Rewriting Eq 3.4 in a normalized form

$$R = \frac{\sigma_{a,2} - \sigma_R(t)}{\sigma_{a,2} - \sigma_{a,1}} = \exp(-kt). \quad \text{(Eq 3.5)}$$

We can introduce a non-dimensional parameter R_σ, called *Residual of Stress Transition*, to conveniently describe the degree of stress transition

$$R_\sigma = \frac{\sigma_{a,2} - \sigma_R(t)}{\sigma_{a,2} - \sigma_{a,1}} \quad \text{(Eq 3.6)}$$

R_σ varies from 1 to 0 for time $t = 0$ to ∞, that is a non-linear mapping of the resistance stress σ_R over $\sigma_{a,1}$ to $\sigma_{a,2}$ for the same period. From Eq 3.5 and 3.6 it comes

$$\ln(R_\sigma) = -kt \quad \text{(Eq 3.7)}$$

With this simple expression we can measure k experimentally: with the use of strain rate jump test (step test) initially developed by Backofen et al. (Ref 40) we can observe the stress transition from one steady-state to another. The kinetic constant k then can be experimentally determined based on R_σ evolution over time. Note that due to the logarithmic form of Eq 3.7 there is no need to completely release the stress to zero; R can be summed incrementally, i.e., $\ln R = \sum_i \ln(R_i) = -k \sum_i t_i$.

The contribution of the stress transition to the total creep rate is complex. Following the classical works (Ref 22-24) where the total creep rate was treated as the sum of forward steady-state rate and backward transient creep rate due to anelastic recovery from a stress drop (Ref 18-20), here we replace the transient anelastic recovery term by transient rate increase due to the driving force $(\sigma_a - \sigma_D)$ while neglecting the anelastic effect. We further assume that the primary creep rate also can be described by a similar power-law rate equation; the total strain rate can be expressed as

$$\dot{\varepsilon} = \dot{\varepsilon}_{pri} + \dot{\varepsilon}_{ss} = C(\sigma_a - \sigma_R)^N + C\sigma_a^N \quad \text{(Eq 3.8)}$$

Here the primary (transient) creep term in Eq 3.8 diminishes upon completion of a transition period. Note that the constitutive model for the primary creep at large plastic deformation has not been fully explored at this time, the current simplification treatment is purely empirical. For achieving present task to investigate the significance of primary creep on tube gas-forming process this treatment is necessary and may be acceptable.

The total creep rate, based on Eq 3.4 and 3.8, can now be expressed as

$$\dot{\varepsilon}(t) = C\sigma_{a,2}^N \pm C'|\sigma_{a,2} - \sigma_R|^{N'} = C\sigma_{a,2}^N \pm C'|\sigma_{a,2} - \sigma_{a,1}|^{N'} \exp(-kt) \quad \text{(Eq 3.9)}$$

The negative sign applies to the case of stress decrease $(\sigma_{a,2} < \sigma_{a,1})$. The use of absolute value for the stress difference can avoid negative base in the power-law formulation. In the case of stress decrease, in addition to the elastic unloading, the creep deformation may either slow-down or change in the direction to backward creep (strain recovery), depending on the magnitudes of the two strain rate terms. This unloading process will not be discussed in this paper.

4. Experimental Determination of Kinetics of Transient Creep

4.1 Experimental Procedure

Tensile test at elevated temperatures were performed for a magnesium alloy, AZ31 (Mg-3 wt.%Al-1 wt.%Zn). The tensile specimens were cut from hot-extruded tubes of 50.4 mm outer diameter and 2 mm wall thickness (nominal dimension), along the tube longitudinal direction. The specimens were machined to "dog-bone" shape with a 10 mm gauge length and 5 mm width, and the thickness was curved as it was in the tube form. The specimen hung on the upper grip without constraint during heating, and the tensile load was applied on the specimen shoulder region, so that there would be no compression force possible on the specimen during heating. Between the specimen gauge section and the shoulders there is a 2 mm radius for transition to avoid stress concentration, and due to excellent superplasticity of the material, no specimen was fractured from the shoulder corner.

Tensile tests were conducted on an Instron 8801 servo-hydraulic material testing machine that has a total capacity of 100 kN, but for the present testing at elevated temperature a small load cell of 10 kN full scale was used to increase the resolution. Due to sufficiently high stiffness of the machine at much reduced load, and also due to very large elongation obtained (in the range of 100-200%), the extension of the specimen was directly measured from Instron's build-in LVDT without an extensometer. The Instron was close-loop controlled with a digital controller under displacement control mode. The signal conditioner of the controller/data acquisition system allows further amplifying the signal to rescale 5% of full scale (or 500 N) into 10 V output. For obtaining transient stress in this study, a data recording rate of 100 Hz was used, which is sufficiently high as compared with the transient stress chance during loading/recovery (that was found in the range from a few seconds to several minutes, depending on the testing temperature and applied load (stress) or speed (strain rate)). The total stroke of the machine is 150 mm.

A vertical split furnace with electrical resistance heating was used. The temperature was controlled within 2 K of the set temperature by a programmable controller and two K-type thermal couples, one for monitoring specimen gauge temperature and another for furnace temperature control. To reduce specimen preheating time that may cause microstructural change, the grips were first preheated to the testing temperature without specimen, and after temperature was ready the specimen was placed inside the furnace by hanging the shoulder on the upper grip and engaging, but not contact, with the lower grip. Further heating and stabilizing the temperature typically took about another 10 min. The tensile tests were conducted at 623, 673, and 723 K, which are in 0.70-0.81 T_m of the material melting point in K. Steady-state creep behavior of AZ31 (Ref 29), and microstructure/texture evolution during deformation that will contribute to current transient creep at material level, were previously studied from sheet materials (Ref 41-43).

Strain rate jump tests (step tests) were conducted by periodic change of displacement rates, the method developed by Backofen (Ref 40) primarily for obtaining materials' strain rate sensitivity (m-value) but in the present study for obtaining materials' transient behavior upon speed changes. Within one-step test a single specimen was stretched under several speeds under Instron's displacement-control mode. Within one segment of strain the load increased as the displacement was activated, and it stabilized at a peak value as the indication of steady state, and it was decreasing with time when the machine stroke was stopped. After majority of the load was released (but not necessarily completely relaxed to zero) a new segment of strain was applied at a different displacement rate. The constant speeds used are at six levels, i.e., 1, 0.5, 0.1, 0.05, 0.1, and 0.005 mm/s that correspond to the strain rates in the order of 10^{-4} to 0.1 s^{-1} but for the same speed the true strain rate slightly varies with instantaneous gauge length, based on the formula $\dot{\varepsilon} = V/l$ where V is the displacement rate and l is the instantaneous gauge length. Figure 1(b) shows the definition of segment, cycle, and step up/down to be specified in the label of segment. In each test the segment started at the highest speed, and reduced step by step to lower levels till at 0.005 mm/s, and then it changed step by step from low to high to complete one cycle, then the whole cycle repeated for again until failure. The segments are labeled by their speed level (the first digit), followed by the cycle number (1 or 2), followed by a letter "u" or "d" indicating the speed was step up or step down, despite that all segments were exclusively loaded after a stress relaxation period. The reason to release the internal stress first is to allow a longer stress transition period at a higher stress change, so the observation of stress transition during loading can be made more easily. Only loading portions are of current interest, because in tube gas bulge forming the applied stress keeps increasing even under a constant internal gas pressure. Multiple step segments within one specimen were possible due to excellent superplasticity of the material at the testing temperatures. The recorded load and displacement over time then provide information on stress transition between associated steady-state stresses.

4.2 Results

The true stress and strain vs. time and the stress vs. strain curve at 723 K are shown in Fig. 1. It can be seen that in the first segment the increase of stress was not smooth, due to specimen self-alignment. By holding the position, the load exponentially dropped down. Each new segment started with rapid load increase and then, after a peak load was reached, the load may still slowly increase, for the first few segments, probably still related to continuous break down of initial microstructure. In those later segments, the stress immediately decreases after a peak stress was reached, which is related to the neck formation and the measured stress based on uniform deformation underestimates the real material flow stress. But, for the purpose of studying the transient load change we still included some of these segments (except for the first segment and very last few segments). The same step-test procedure was used for 673 and 773 K tests, but the total number of segments used was less.

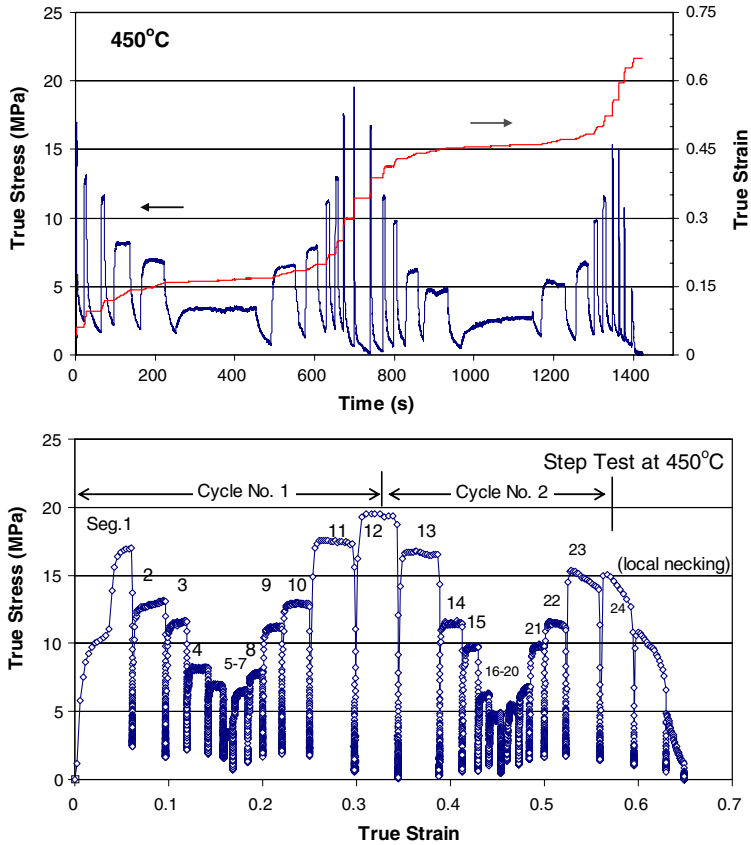

Fig. 1 Strain rate step test at 450 °C. Similar tests were performed at 400 and 500 °C as well. The data of position and load were taken at sampling rate of 500 Hz. Each plotted data points were the average of 50 recorded points

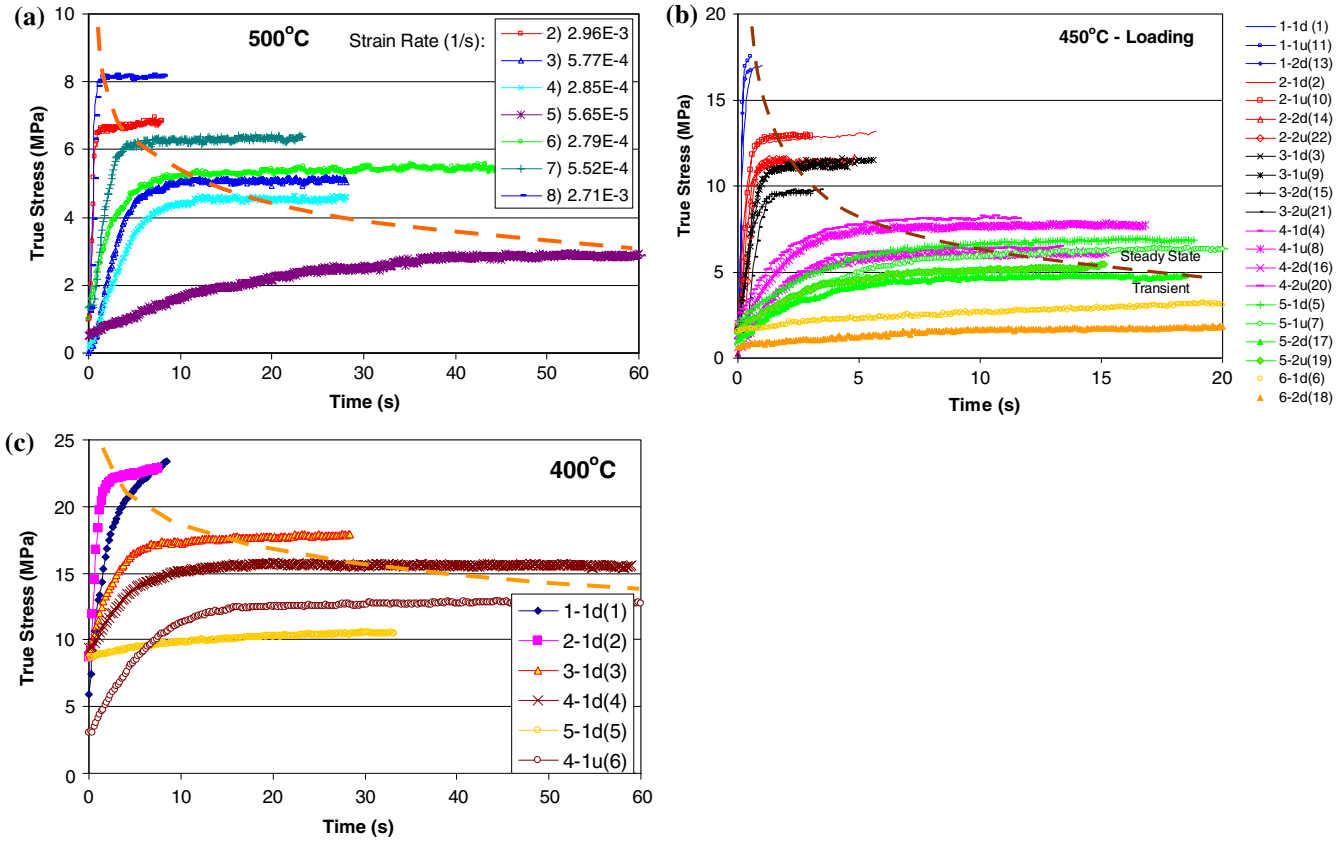

Fig. 2 Transient stress transition during strain rate change in the step tests of Mg AZ31 at 500 °C (a), 450 °C (b), and 400 °C (c), with the time reset at zero from the time of strain rate change. The labels of the curves are noted to indicate the velocity (first letter), step cycle number (cycle 1 or 2 from strain step-down ("d") or step-up ("u") within the cycle, and the series segment number in bracket). For example, "6-2d(18)" means velocity level 6 (0.0005 mm/s) in the second cycle with speed step-down, in Segment 18 (see Fig. 1b)

For each strain segment, the true stress vs. time portion was taken and, by resetting the time zero at the beginning of each segment upon loading, all the loading curves are shown in Fig. 2 for three temperatures, respectively. For all curves, the stress first increased rapidly, then the increase slowed down and finally a steady-state stress was reached (or almost reached). With the increase of speed the steady-state stress increases, so does the rate of stress increase. The time to reach the steady state varies with the speed change or steady-state stress; see the dashed line for schematic representation. The transition time was roughly in the range from 2 s to more than a minute depending on the speed or corresponding steady-state stress—it is shorter for a higher speed and temperature.

In order to obtain the kinetics of transient stress development during loading, the stress vs. time data in Fig. 2 are converted to the residual of stress transition, R_σ defined by Eq 3.6, and re-plotted against time, see Fig. 3. All the curves start from 1 and decrease with time at decreased rate. By further changing the y-axis to logarithm scale for R_σ the curves then show almost linear relation with time, so the kinemics equation Eq 3.7 is generally satisfied. As an example Fig. 4 shows that R_σ has exponential relationship with time t, and for other two temperatures the situation is the same (but the plots are very crowded and not shown here). Note that below $R_\sigma = 0.05$ or 0.1 this exponential relationship no more exists, which is understandable because in reality the stress transition time does not go to infinity but can reach a steady state with a finite time, in disagreement with the model suggestion.

The slopes of all these curves within 90% completion of the stress transition are plotted in Fig. 5. It can be seen that the k-value increases with the amount of stress change, and with the temperature. A best-fit exponential equation was obtained for each temperature, as shown in the figure. Good correlation coefficients ($R^2 > 0.9$) were obtained for all three temperatures. A higher k-value means a higher stress transition speed or shorter transient time. It is worthy noting that here the stress transition occurred from a stress-free relaxation condition to a loading condition at a much higher stress change, as compared with that in tube gas-forming process, where the applied stress gradually and continuous increases with deformation. This experimental result shows that the transient time varies in 3-100 s, corresponding to the k-values in the order of 1-0.001.

To analyze the transient creep in the previous tensile tests, the kinetic model in Section 3 is used for computing the internal creep resistance σ_D and from that obtaining the strain rate, as shown in Fig. 7. With the assumption that the same power-law rate equation and material constants are applied for the primary creep rate equation but with the net contribution from the difference between the applied stress and the internal creep resistance, which increases from zero (for initial stress-free condition) towards the applied stress, the primary strain rate term would be the same to the steady-state term initially and gradually reduces to zero. The rate to approach zero is controlled by the k-value, which takes longer time for a lower k-value, so the primary creep contributes more to the total strain.

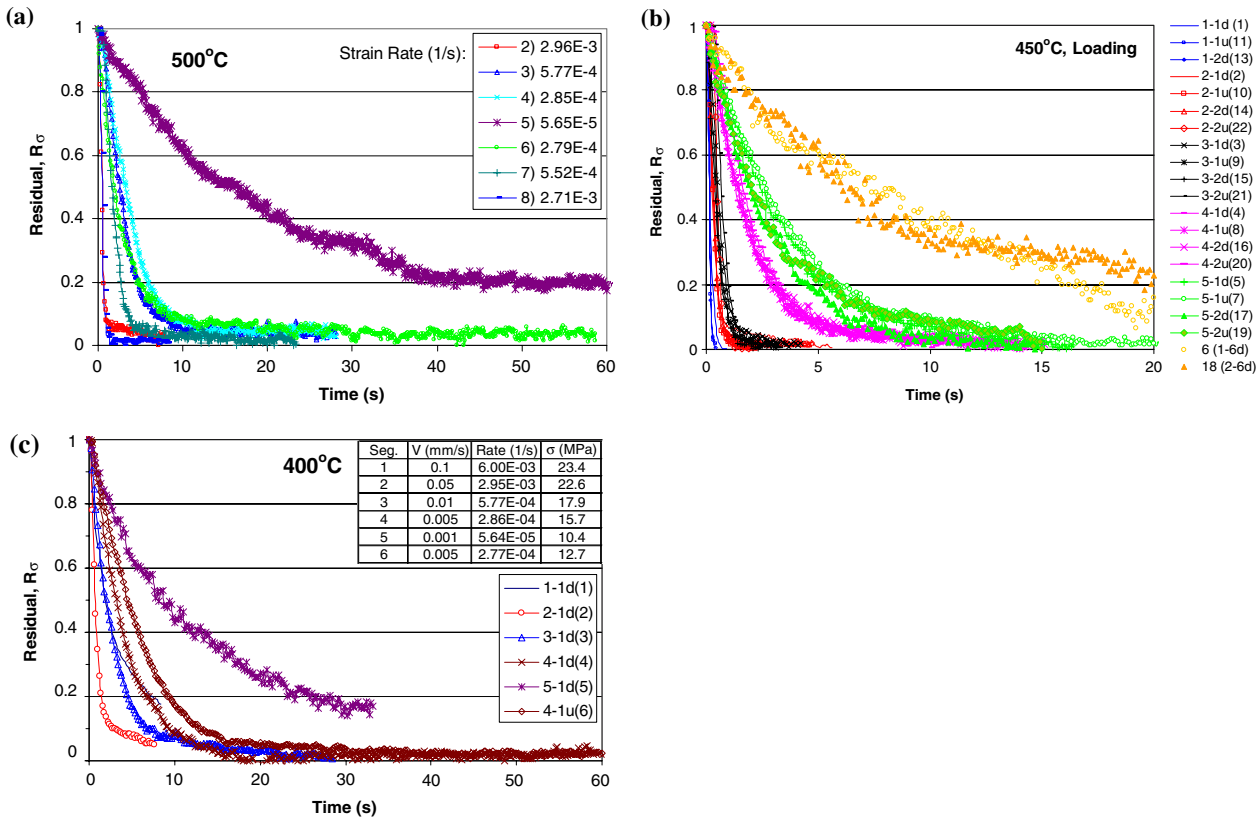

Fig. 3 Residual factor R_σ of stress transition upon strain rate changes, at 500 °C (a), 450 °C (b), and 400 °C (c)

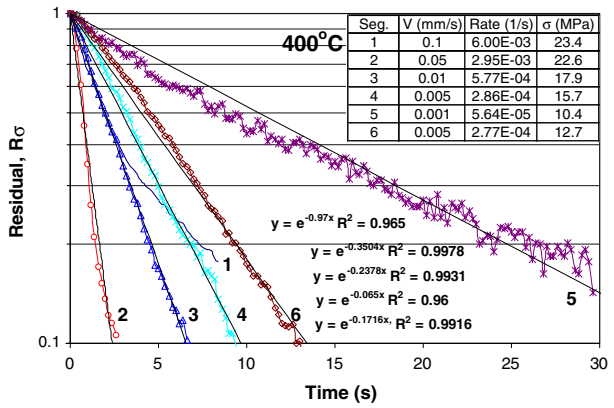

Fig. 4 Residual factor of stress transition, from strain rate step test of Mg AZ31 at 400 °C, plotted in semi-log scale

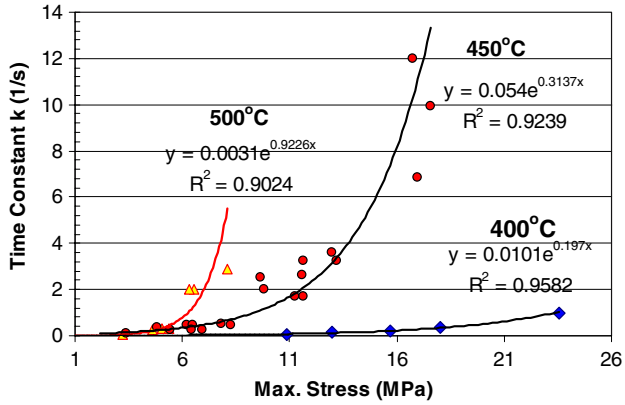

Fig. 5 The time constant k vs. the maximum stress appeared in strain rate step test, for 500, 450, and 400 °C, respectively. An exponential regression was used for the observed non-linear relationship

5. Transient Creep in Tube Expansion

In this section the mechanics of tube forming is given first, and then the effect of transient creep on tube expansion process is analyzed.

5.1 Mechanical Analysis of Tube Expansion with Transient Creep

The schematic of stress state in tube expansion is shown in Fig 7. Based on classical plasticity theory [see Hosford and Caddell (Ref 44)], the three principle strains in a tube forming, the hoop strain ε_1, axial strain ε_2 and radial (thickness) strain ε_3, are expressed in terms of tube geometry changes (radius r, length l, and wall thickness h),

$$d\varepsilon_1 = d\varepsilon_\theta = \frac{dr}{r}, \quad \text{and} \quad \varepsilon_1 = \ln\frac{r}{r_0} \qquad \text{(Eq 5.1)}$$

$$d\varepsilon_2 = d\varepsilon_x = \frac{dl}{l}, \quad \text{and} \quad \varepsilon_2 = \ln\frac{l}{l_0} \qquad \text{(Eq 5.2)}$$

$$d\varepsilon_3 = d\varepsilon_h = \frac{dh}{h}, \quad \text{and} \quad \ln\frac{h}{h_0} \qquad \text{(Eq 5.3)}$$

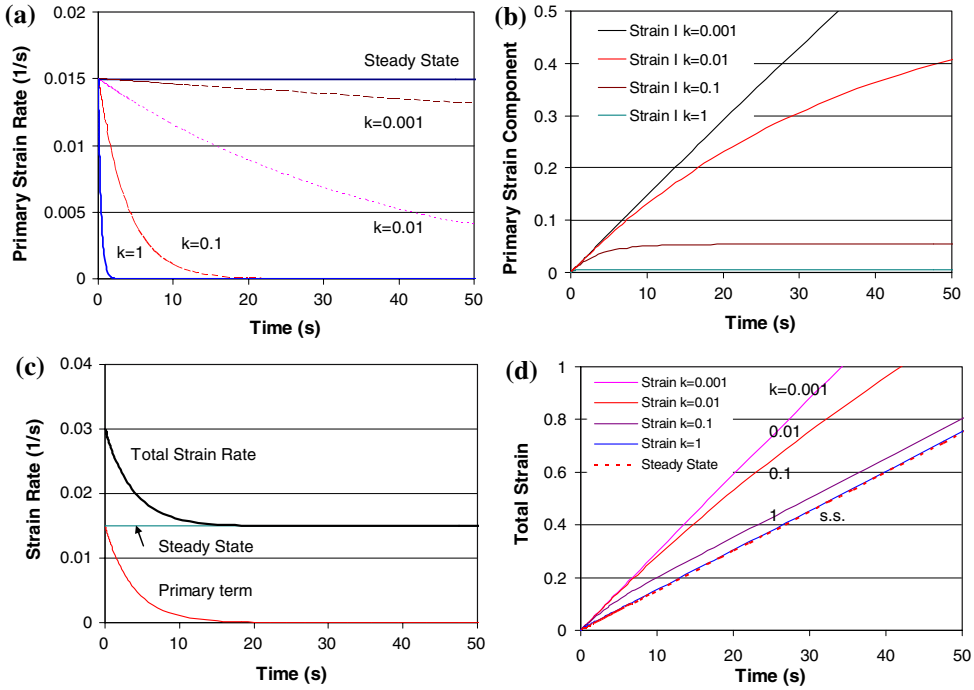

Fig. 6 Calculated strain rate and strain considering primary (transient) creep, based on Eq 3.7 and with the steady-state material parameters for Mg AZ31: $C_0 = 25439.95$, $N = 2.60$ ($m = 0.385$), $Q = 145$ kJ/mol, and $T = 450$ °C [from (Ref 39)]. The primary strain rate diminishes after a transition time, which decreases with increasing time constant k (a). The primary strain increases with transition time or decreasing k (b). The total strain rate is the sum of the primary (transient) and secondary (steady-state) terms (c). The primary creep becomes more important to the total strain for lower k values (d)

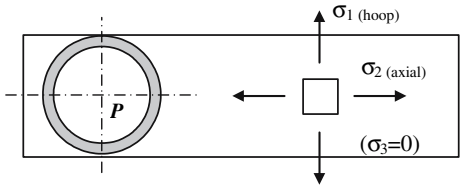

Fig. 7 Stress components in tube forming

From volume conservation in plasticity

$$\dot{\varepsilon}_1 + \dot{\varepsilon}_2 + \dot{\varepsilon}_3 = 0 \qquad \text{(Eq 5.4)}$$

Assuming von Mises Yield criterion and with the normal stress $\sigma_3 = 0$ for thin-wall tube,

$$\sigma_1^2 - \sigma_1\sigma_2 + \sigma_2^2 = Y^2, \qquad \text{(Eq 5.5)}$$

where Y is the yield stress. The stress ratio and strain rate ratio are defined as,

$$\alpha = \frac{\sigma_2}{\sigma_1} \quad \text{and} \quad \beta = \frac{\dot{\varepsilon}_2}{\dot{\varepsilon}_1} = \frac{\Delta\varepsilon_2}{\Delta\varepsilon_1} \qquad \text{(Eq 5.6)}$$

Based on Levy-Mises flow rule the two ratios are related by

$$\alpha = \frac{2\beta + 1}{2 + \beta} \quad \text{or} \quad \beta = \frac{2\alpha - 1}{2 - \alpha} \qquad \text{(Eq 5.7)}$$

From the radial force equilibrium, the hoop stress for a thin-wall tube can be given by

$$\sigma_1 = P\frac{R}{h}, \quad \text{where} \quad R = \left(\frac{1}{R_1} + \frac{1}{R_2}\right)^{-1} \qquad \text{(Eq 5.8)}$$

where R is the effective radius of two in-plane principal curvatures R_1 and R_2. Thus, von Mises effective stress can be expressed by the major principal stress as,

$$\bar{\sigma} = (1 - \alpha + \alpha^2)^{1/2}\sigma_1 \qquad \text{(Eq 5.9)}$$

With the gas pressure wavefunction and strain/stress path given, the applied effective stress σ and the transient stress σ_T can be updated depending on kinetic constant k and elapsed time. Since in tube forming under a constant gas pressure the applied stress is increasing with time, $\sigma_a(t)$ is not constant, so we have to use the incremental form of the transient stress, from Eq 3.1,

$$\sigma_R(t + dt) = \sigma_R(t) + \dot{\sigma}_R(t)dt = \sigma_R(t) + k[\sigma_a(t) - \sigma_R(t)]dt \qquad \text{(Eq 5.10)}$$

and initially $\sigma_R(0) = 0$. The effective strain rate can be obtained from the previous model,

$$\dot{\bar{\varepsilon}} = C\sigma^N + \delta C(\sigma - \sigma_D)^N \quad (\delta = 0, 1) \qquad \text{(Eq 5.11)}$$

where $\delta = 0$ for steady-state creep (without considering transient creep) for comparison, and $\delta = 1$ for including transient creep. The principal strain rate components are

$$\dot{\varepsilon}_1 = \left[\frac{4}{3}(1 + \beta + \beta^2)\right]^{-0.5} \cdot \dot{\bar{\varepsilon}} \qquad \text{(Eq 5.12)}$$

$$\dot{\varepsilon}_2 = \beta\dot{\varepsilon}_1 \qquad \text{(Eq 5.13)}$$

$$\dot{\varepsilon}_3 = -(1+\beta)\dot{\varepsilon}_1 \qquad \text{(Eq 5.14)}$$

Accordingly the strain increment and total strain can be obtained/updated by,

$$\Delta\varepsilon_j = \dot{\varepsilon}_j \Delta t \quad \text{and} \quad \varepsilon_j := \varepsilon_j + \Delta\varepsilon_j \quad (j = 1, 2, 3) \qquad \text{(Eq 5.15)}$$

Thus, the tube radius, length and wall thickness are ready to be determined.

$$r = r_0 \exp(\varepsilon_1), \quad l = l_0 \exp(\varepsilon_2), \quad \text{and} \quad h = h_0 \exp(\varepsilon_3) \qquad \text{(Eq 5.16)}$$

This allows updating the hoop stress based on the new (r/h) ratio for next time increment. For a given strain/stress path (constant α and β) the iteration from Eq 5.8-5.16 continues for each incremental time until a specified criterion is reached. For simplicity here we define an instable tube expansion condition as that when the relative change of strain rate from one time increment $\gamma = \Delta\dot{\bar{\varepsilon}}/\dot{\bar{\varepsilon}}$ [i.e., $\dot{\bar{\varepsilon}}(t+\Delta t)/\dot{\bar{\varepsilon}}(t) - 1$, also $\Delta d\varepsilon/d\varepsilon$] reaches a critical value γ_{cr}, which is adjustable based on experimental data.

5.2 Computation Results

The calculated strain development during tube expansion is shown in Fig. 8 for tube dimension of $r_0 = 25$ mm and $h_0 = 2.5$ mm, under plane strain condition ($\beta = 0$). Material creep properties are (based on previous experimental study on steady-state creep of Mg AZ31): $m = 0.385$, $C_0 = 25439.95^{1/m}$ s^{-1}, $Q = 145$ kJ, $T = 723$ K, $p = 2$ MPa, and the transient creep time constant $k = 0.1$. The result is within the range of lab tube gas-forming condition. In this forming process, the radial strain and thickness strain develop steadily in majority of the early forming process but the deformation accelerates rapidly at last few seconds. This plot represents general feature of tube expansion process.

The choice of time increment size dt may give different results on tube instable expansion. To verify the effect of time increment, three dt values, 0.1, 0.01, and 0.001 s were used for comparison, and the relative strain change $\gamma = \Delta\dot{\bar{\varepsilon}}/\dot{\bar{\varepsilon}}$ is plotted over forming time t, as shown in Fig. 9(a). From local enlargement in logarithm scale it can be seen that indeed the three dt provided different transition to the instability or γ curves, with smaller dt producing sharper instability at the very end of the forming. However, in terms of final strain, see Fig. 9(b), all the three time increments produced almost identical total strain. We used $dt = 0.01$ s for all other simulation in this paper, so that the error from numerical part will be systematic and relative.

To determine the instability criterion γ_{cr}, it needs to verify the impact of critical strain development, γ to the limit strain condition. Figure 10 plots both γ and effective strain ε vs. time t. In view $\varepsilon(t)$ curve it is found that γ always increases with time, as the result of monotonically increasing r/h. This is consistent with the accelerated strain development shown in Fig. 7. The current $\log(\varepsilon)$-t plot indicated that it always has a positive slope, or $d(\log\varepsilon)/dt > 0$. However, the slope is decreasing first (or say the second derivative $d^2(\log\varepsilon)/dt^2 < 0$) and then at certain turning point $d^2(\log\varepsilon)/dt^2 = 0$ and after that it turns to positive. Since $d(\log\varepsilon)/dt = \dot{\bar{\varepsilon}}/\varepsilon$, it represents the competition between strain rate development and total strain development: if $\dot{\bar{\varepsilon}}/\varepsilon$ decreases with time that means strain development is faster than strain rate development, so the deformation is stable; otherwise it is less stable. It is well known that although structural instability of pressurized tube can be convenient to be analyzed, localized necking occurs much later than the maximum pressure so it can not be used for limit strain prediction in tube manufacturing. From Fig. 10, the choice of γ_{cr} should avoid being too close to the final instability region, otherwise it will be too sensitive in predicting the total limit strain. It is found that γ developed rather slowly as

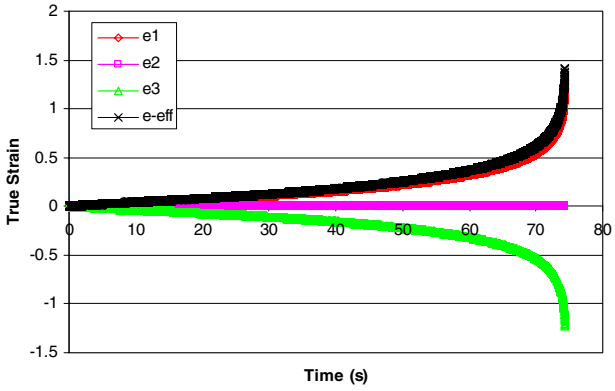

Fig. 8 Strain development in tube gas bulging at elevated temperature, from simulation under the condition: Tube dimension of $r_0 = 25$ mm and $h_0 = 2.5$ mm, under plane strain condition ($\varepsilon_2 = 0$). Material creep properties are (based on Mg AZ31): $m = 0.385$, $k = 0.1$ s^{-1}, $T = 450$ °C, and $p = 2$ MPa

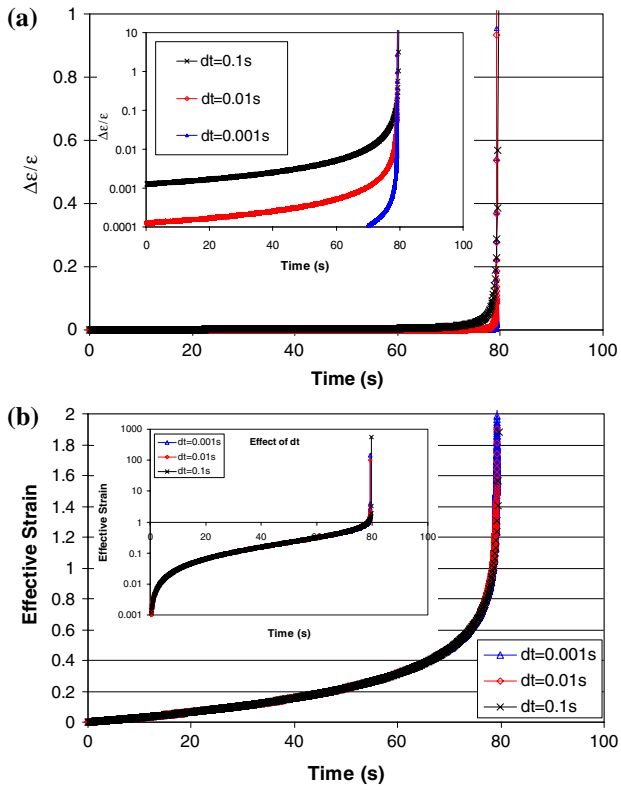

Fig. 9 The effect of time increment dt on the convergence of the computing results, computed at $k = 0.01$ s^{-1}. Larger dt does affect the determination of critical strain rate ratio (a), but it has limited effect on computed effective strain (b). The insets are in log-scale for y-axis to show broader range

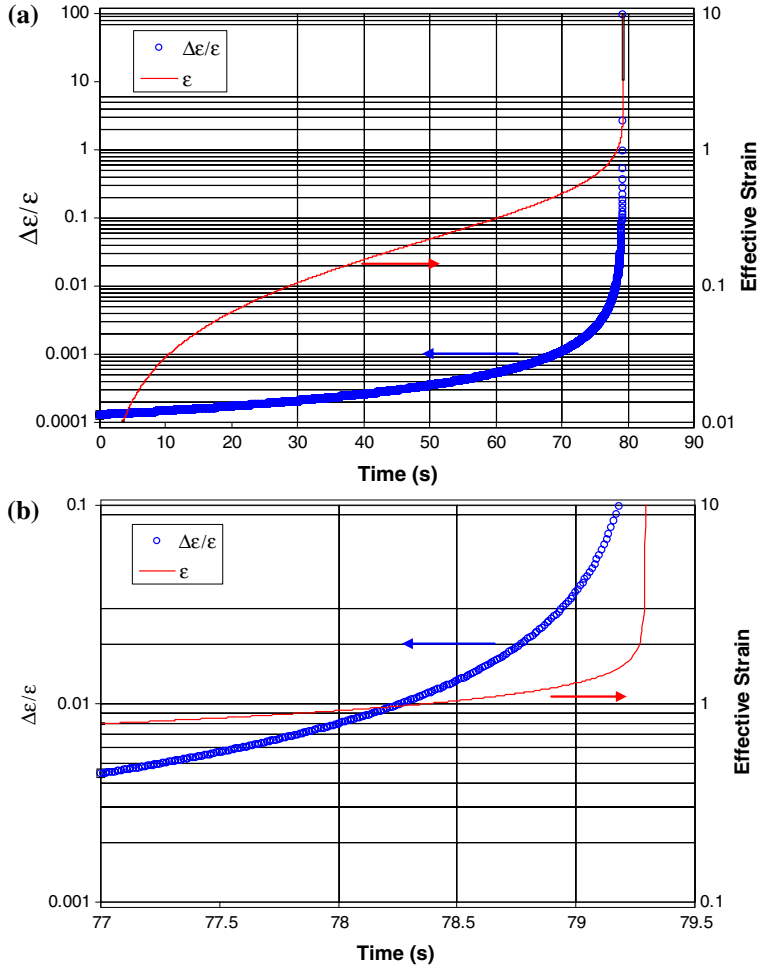

Fig. 10 The strain development process can be viewed from the relationship between relative change of strain increment and the total effective strain

compared with strain development; even at $\gamma = 0.01$ (or 1% increase in relative incremental strain) the total strain already closes to 1. This gives a good opportunity to use γ within its stable development region to indicate the degree of unstable development of total strain. The laboratory final expansion ratio on plane strain tube free expansion is in the range of 0.5-0.8. Besides many disturbance factors such as initial tube defects (especially wall thickness inhomogeneity) and circumferential temperature variation, the intrinsic mechanical instability of tube expansion may provide a foundation and theoretical window on tube forming. In practical application γ_{cr} can be empirically fitted from experimental data. Unlike instability of flat sheet metals, the criterion on limit strain in tube forming received many debates and it deserves further investigation (but will not further expand here).

The effect of transient creep kinetics on the strain development is shown in Fig. 11, for k-values from the magnitudes of 0.001 to 10, with all other forming conditions remained the same. The steady-state creep condition (without considering transient creep term) is also included as a reference. It is seen that final strains from different k are about the same to that in steady-state creep, since here we used the same strain rate sensitivity for both transient creep and steady-state creep. However, the forming time changes significantly: the steady state alone without transient creep gives slowest forming process, and at high k-values ($k = 10$ and $k = 1$) there is limited reduction of forming time. From $k = 0.1$ to 0.01 there is significant reduction of forming time.

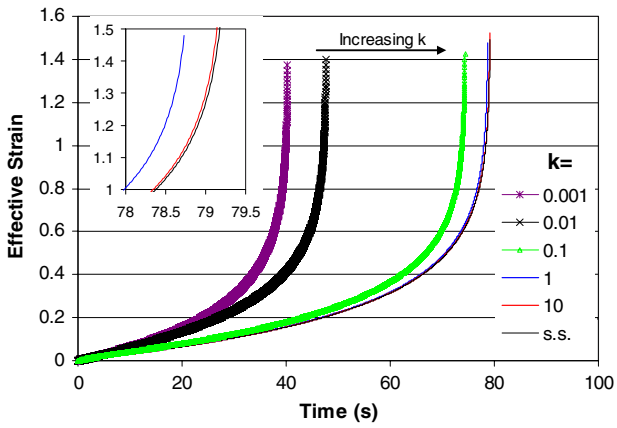

Fig. 11 Effective strain development during gas bulging for various transient kinetic parameter k (= 0.001, 0.01, 0.1, 1, and 10 s^{-1}), along with that for steady-state creep result without considering transient creep (at the right-most line). The inset shows local enlargement

To interpret these results, the total strain is controlled mainly by material rate sensitivity. In the current simulation, without sufficient knowledge on primary creep equation the same material parameters were for both steady state and transient creep formulation, in which *m*-value is known to have significant impact to necking development but it was unchanged for both steady state and transient creep formulations. This explains why there is limited difference of instable strain development. The forming time is controlled by the strain rate, to which the primary creep has significant contribution, as shown previously both from experimental observation and theoretical analysis. However, the role of transient creep on tube forming is rather complex, as seen in the non-linear relationship of *k* value and the forming time reduction in the figure.

To reveal the kinetics in transient stress development, both applied stress and the internal resistance stress development during tube expansion are shown in Fig. 12. The applied stress is solely controlled by the amount of strain, or more exactly the ratio of *r*/*h* (for forming under a constant pressure and plane strain condition). The transient stress, on the other hand, depends on both applied stress development and the time required for the internal resistance stress to catch up with the applied stress. Three cases exist in regarding with *k*-values, with a reference total gas tube-forming time of 10-100 s:

(a) At high *k* regime ($k > 0.1\ s^{-1}$) the transient stress development is fast enough to catch up with the change of applied stress caused by the increasing *r*/*h* ratio during tube gas forming. There is limited or no contribution of transient creep to total deformation, so the tube-forming process can be well described by steady-state creep alone;

(b) At low *k* regime ($k < 0.01$) the transient stress development is too slow to catch up with the applied stress (initially) and its changes (later stage), so that the tube deformation is under significant effect of transient creep. As a result the total creep rate is much higher than that in steady-state condition, resulting in significant reduction of forming time.

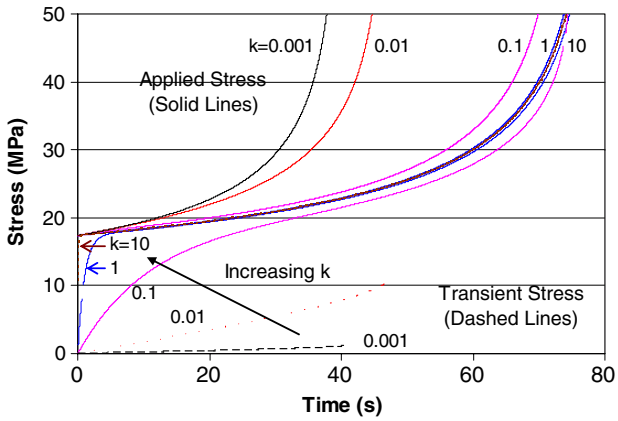

Fig. 12 Transient stress development during tube gas bulging for various kinetic parameter *k* (= 0.001, 0.01, 0.1, 1, and 10 s^{-1})

(c) At intermediate *k* regime (*k* from 0.01-0.1) the rate of transient stress development is in the same order of magnitude to the rate of applied stress increase, the latter is accelerating during tube expansion. Thus, at early stage of forming the difference between the applied stress and the internal resistance is reducing with deformation, but at later stage of forming the difference increases again. Accordingly, the transient creep contributes the total creep rate increase at both early and later stages of tube forming but has reduced or no contribution in middle portion of the forming. In this intermediate *k* regime the kinetics of transient stress development has sensitive effect to the deformation process. Apparently the current hot metal gas-forming process is right in this regime.

6. Discussion

6.1 On Experimental Validation of Transient Creep

At this time the direct experimental validation of the above computed results are not available, due to the following difficulties encountered:

(a) The material creep model obtained from tensile test along the tube longitudinal direction can not reflect a hoop deformation-dominated tube expansion process. The previous study indicates that strong crystallographic texture exists in almost all the available tubes made either from extrusion (for aluminum and magnesium alloys) or from rolling and roll-forming of steel sheets.

(b) In our direct measurement of radial displacement during tube expansion it was found difficult to make clear distinction between primary creep and secondary creep, and between plastic strain and anelastic strain from continuous increase of gas pressure. Even with step change of applied pressure or temperature that enlarges the change of applied stress, the measured transient tube expansion always combines intrinsic material transient creep and transient mechanical system/temperature change (associated with the use of gas pressure and heat transformation). Further improvement of signal-to-noise ratio under a high magnetic field from induction heating unit is also needed. A new tube creep testing technique to resolve these issues is needed.

6.2 Tube Forming Along Other Strain Path

In the present computation only plane strain condition is considered. For other strain paths it is expected that the general feature of transient creep will still apply but only with some magnitude changes on the forming rates. The transient stress development is caused by the change of applied (effective) stress, which is related to the 3D deformation mode and can be completely described by a single parameter, the strain path β. In review of applied stress evolution during tube deformation, which is dictated by the ratio of *r*/*h*, we can use a normalized expression of ratio *r*/*h* per unit strain to evaluate the effect of strain path β on transient creep. Since

$$\frac{r}{h} = \frac{r_0}{h_0}\exp[(2+\beta)\varepsilon_1] = \frac{r_0}{h_0}\exp\frac{(2+\beta)\varepsilon}{\sqrt{(4/3)(1+\beta+\beta^2)}} \quad \text{(Eq 6.1)}$$

the value of (r/h) can be related to β in its logarithm form with a normalizer (r_0/h_0), per hoop strain or effective strain,

$$\frac{1}{\varepsilon_1}\ln\left(\frac{r/h}{r_0/h_0}\right) = 2+\beta \quad \text{(Eq 6.2)}$$

$$\frac{1}{\varepsilon}\ln\left(\frac{r/h}{r_0/h_0}\right) = \frac{(2+\beta)}{\sqrt{(4/3)(1+\beta+\beta^2)}} \quad \text{(Eq 6.3)}$$

These two equations have the same meaning in terms of (r/h) development per unit strain, but for the strain development they use different forms, as shown in Fig. 13. For unit effective strain the value (r/h) is highest at $\beta = 0$, and it is lowest at $\beta = 1$ and $\beta = -0.5$, both at 86.6% of the maximum. With respect to the hoop strain ε_1 the r/h development is the highest at $\beta = 1$ and the lowest at $\beta = -0.5$ (50% of the maximum). This is related to the reduced thinning at a lower β. Therefore, if based on effective strain development, the current computation results under plane strain condition gives the highest hoop stress development rate, which is the fundamental reason for applied stress increase during hot tube gas forming.

6.3 A Further Discussion on Transient Kinetics of Materials

In Section 2 the transient stress change rate was treated proportionally to the difference between applied and internal stresses. This assumption is purely from kinetics consideration and did not consider any mechanisms that are responsible for the kinetic transfer so that they may affect the time constant k. From thermodynamic point of view k may not really be a constant. The experimental results shown in Fig. 5 already indicate that k is not only a function of temperature but the stress change as well. Since the creep deformation is a diffusion process involving dislocation motion and mass transportation under various paths, the kinetics of stress evolution should also

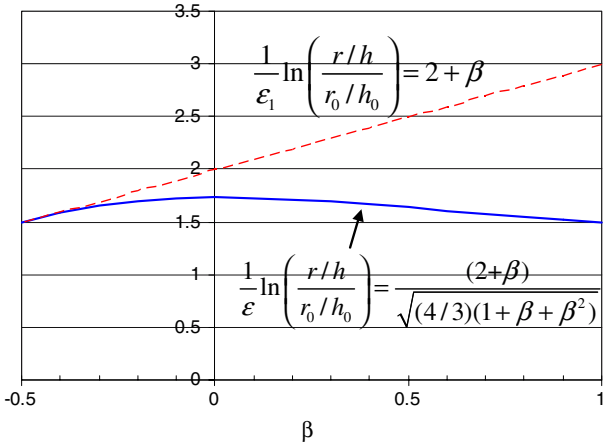

Fig. 13 The effect of strain path β on non-steady-state tube deformation. The normalized $\ln(r/h)$ per unit strain is used to relate β to hoop stress development per unit strain (either effective or hoop strain). A higher y-value means more significant increase of hoop stress per unit strain, so the deformation is less steady

be a thermodynamic parameter. A thermodynamic expression for the kinetic constant k may be written as

$$k = k_0\exp(\lambda\Delta\sigma - Q/RT) = k_0\exp(\lambda\Delta\sigma)\cdot\exp(-Q/RT) \quad \text{(Eq 6.4)}$$

where $\Delta\sigma$ is the difference $(\sigma_a - \sigma_D)$, and λ is a material-dependent prefactor. This indicates that both thermal activation term and stress term $\exp(\lambda\Delta\sigma)$ contribute to the kinetics of transient, or to the time constant k. This provides a support to use an exponent law for the stress dependence of k, shown in Fig. 5.

In this paper we did not discuss the relaxation behavior; however, from Fig. 1(a) it is obvious that the kinetics for stress relaxation was at a much lower speed—the transition time for stress relaxation is much longer than that in loading. This is another reason in the tensile tests we tried not to involve both loading and unloading cases but all the results shown here were from loading up condition (after a stress relaxation period). During stress relaxation process there is no assistance for internal resistance received from external stress, and what being measured on the graceful external load drop is the internal stress itself. But under this displacement-constrained condition the stress transient process should be different from that under a constraint-free condition. Further study on both loading and unloading processes, and under load and displacement controlled modes are of future interests.

In this paper the effect of transient creep is analyzed for hot tube gas forming only, and this process has its intrinsic trend of applied stress increase under a constant gas pressure. For other hot deformation processes the necessity for changing applied stress is not so clear, so that the effect of transient creep on deformation is less obvious. On the other hand, if consider that almost all thin-wall component forming (e.g., thin sheet hot forming by gas or by punch) would involve reduction of wall thickness and enlargement of surface area, the systematic increase of applied stress would also exist in a very similar fashion to that in tube expansion. For these processes, whether the transient creep needs to be considered really depends on the comparison between the time scale of forming process and the time scale of material's primary creep regime at the forming temperature and applied stress (or strain rate). Based on the finding given in Section 5 that shows three distinct regimes of transient effects, if material's primary creep period is much shorter than the forming time, there is no need to consider transient effect, otherwise it does. When the two time scales are in the same magnitude special care needs to be taken of to address the sensitivity of transient effect on the forming process. In this sense, the current finding applies to both high-speed forming as well as low-speed one, as long as there exists a significant change in applied stress during forming.

7. Conclusions

Much of previous works on elevated-temperature metal-forming processes consider steady-state creep only and transient creep is neglected for simplicity. This is an initial investigation and assessment of the effect of transient creep on one of the high-temperature deformation processes, hot metal gas forming. The kinetics of transient creep and its effect on tube deformation process has been studied, and the following results and conclusions are drawn:

(1) A transient material creep model is developed based on the kinetics internal resistance evolution. A new non-dimensional parameter, the residual of stress transition, was introduced to describe the degree of transient process. This analysis serves as a foundation for experimental design and data processing.

(2) The kinetics of transient stress development associated with applied stress increase was experimentally investigated for an Mg AZ31 tube material at 673, 723, and 773 K, and at strain rates ranging from 10^{-4} to 1 s^{-1}, a window of current hot metal-forming conditions. By using a modified strain rate step test and by introducing a new parameter of the residual of stress transition, the kinetic time constant k as a function of temperature and stress has been obtained.

(3) Tube expansion mechanics based on transient creep model has been analyzed. Three transient creep regimes are identified based on tube gas-forming process that takes 10-100 s: (a) At high k regime ($k > 0.1$ s^{-1}) the transient stress development can catch up with the change of applied stress. There is limited or no contribution of transient creep to total deformation. (b) At low k regime ($k < 0.01$) the transient stress development can not catch up with the applied stress (initially) and its changes (later stage), so that under significant effect of transient creep, there is a significant reduction of forming time. (c) At intermediate k regime (k from 0.01 to 0.1) the rate of transient stress development is in the same order of magnitude to the rate of applied stress increase. The transient creep contributes the total creep rate increase at the early and later stages of tube forming, and the process is sensitive to the k-value. The current hot metal gas forming is right in this regime.

The current study provides a frame work for understanding the importance of transient creep in elevated temperature forming, especially when the strain rate is high. Further study is needed on understanding physical process involved in transient creep, and the development of a phenomenological transient creep model and a suitable tube experimental technique for direct validation of modeling results.

References

1. The Steel Industry Technology Roadmap for Automotive, 08/07/2006. Available for download from website: http://www.autosteel.org/AM/Template.cfm?Template=/Search/SearchDisplay.cfm.
2. M.S. Rashid, C. Kim, E.F. Ryntz, F. Edward, F.I. Saunders, R. Verma, and S. Kim, "Quick Plastic Forming of Aluminum Alloy Sheet Metal," US Patent No. 6,253,588 , July 3, 2001
3. W. Dykstra, G. Phaffmann, and X. Wu, "Method of Forming a Tubular Blank Into a Structural Component and Die Therefore," US Patent No. 6,322,645 B1, Nov. 27, 2001
4. T. Altan "Hot-Stamping Boron-Alloyed Steels for Automotive Parts, Part I and Part II," STAMPING JOURNAL®, http://www.thefabricator.com/PressTechnology/PressTechnology_Article.cfm?ID=1542
5. G. Phaffmann, X. Wu, and W. Dykstra, Hot Metal Gas Forming of Auto Parts, *Adv. Mater. Process.*, 2000, **2**, p H35–37
6. W. Dykstra, G.D. Phaffmann, and X. Wu, Hot Metal Gas Forming – the Next Generation Process for Manufacturing Vehicle Structure Components, *International Body Engineering Conference*, Nov. 2, 1999, SAE Technical Paper Series 1999-01-3229
7. M.F. Ashby and R.A. Verrall, Diffusion-Accommodated Flow and Superplasticity, *Acta Metall.*, 1973, **21**(2), p 149–163
8. J.E. Dorn, *Creep and Recovery.* ASM, Ohio, 1957, 2255
9. J.E. Bird, A.K, Mukherjee, and J.E. Dorn, *Quantitative Relation Between Properties and Microstructure*, D.G. Brandon and A. Rosen, Eds., Haifa University Press, Israel, 1969, p 255
10. G.A. Webster, A.P. Cox, and J.E. Dorn, A Relationship Between Transient and Steady State Creep at Elevated Temperature, *Met. Sci. J.*, 1969, **3**, p 221–225
11. C.N. Ahlquish and W.D. Nix, The Measurement of Internal Stresses During Creep of Al and Al-Mg Alloys, *Acta Metall.*, 1971, **19**, p 373–385
12. P.J. Henderson and M. MeLean, Microstructural Contributions to Friction Stress and Recovery Kinetics During Creep of the Nickel-Base Superalloy in 738LC, *Acta Metall.*, 1983, **31**(8), p 1203–1219
13. G.J. Lloyd and R.J. McElroy, On the Anelastic Contribution to Creep, *Acta Metall.*, 1974, **22**, p 339–348
14. Y. Li, S.R. Nutt, and F.A. Mohamed, An Investigation of Creep and Substructure Formation in 2124 Al, *Acta Mater.*, 1997, **45**, p 2607–2620
15. E.M. Taleff, W.P. Green, M.-A. Kulas, T.R. McNelley, and P.E. Krajewski, Analysis, Representation, and Prediction of Creep Transients in Class I Alloys, *Mater. Sci. Eng.: A. The Langdon Symposium: Flow and Forming of Crystalline Materials*, 2005, **410-411**, p 32–37
16. M.A. Kulas, W.P. Green, E.M. Taleff, P.E. Krajewski, and T.R. McNelley, Deformation Mechanisms in Superplastic AA5083 Materials, *Metall. Mater. Trans. A-Phys. Metall. Mater. Sci.*, 2005, **36A**, p 1249–1261
17. A. Orlova, An Estimate of Internal-Stress Evolution in the Primary Creep Based on the Composite Model of Dislocation-Structure, *Mater. Sci. Eng. A-Struct. Mater. Proper. Microstruct. Process.*, 1993, **163**, p 61–66
18. A. Orlova, K. Milicka, and F. Dobes, Choice of Evolution Equation for Internal-Stress in Creep, *Mater. Sci. Eng. A-Struct. Mater. Proper. Microstruct. Process.*, 1995, **194**, p 9–16
19. J. Montemayoraldrete, A. Mendoza, and E. Orozco, About the Internal-Stress Measurements During Sigmoidal Transient Creep in Cu-16at-Percent-Al, *Mater. Sci. Eng. A-Struct. Mater. Proper. Microstruct. Process.*, 1993, **160**, p 71–79
20. T.L. Dragone and W.D. Nix, Steady-State and Transient Creep-Properties of an Aluminum-Alloy Reinforced with Alumina Fibers, *Acta Metall. Mater.*, 1992, **40**, p 2781–2791
21. Y.M. Wang and G.J. Weng, Transient Creep Strain of a Fiber-Reinforced Metal-Matrix Composite Under Transverse Loading, *J. Eng. Mater. Technol.-Trans. ASME*, 1992, **114**, p 237–244
22. Y.M. Wang, Y.P. Qiu, and G.J. Weng, Transient Creep-Behavior of a Metal Matrix Composite with a Dilute Concentration of Randomly Oriented Spheroidal Inclusions, *Compos. Sci. Technol.*, 1992, **44**, p 287–297
23. K.J. Hemker, M.J. Mills, and W.D. Nix, A Critical Analysis of Existing Models for Plastic-Flow in Ni3al – Comparisons with Transient Deformation Experiments, *J. Mater. Res.*, 1992, **7**, p 2059–2069
24. W.F. Pan and W.J. Chiang, et al., Endochronic Analysis for Rate-Dependent Elasto-Plastic Deformation, *Int. J. Solids Struct.*, 1999, **36**(21), p 3215–3237
25. F. Dobes, The Simulation of Anomalous Transient Creep by Means of Composite Model, *Scripta Metall. Mater.*, 1991, **25**, p 2303–2306
26. F. Dobes, Strain Dependence of the Volume Fraction of Hard Regions in the Composite Model of Plastic-Deformation and Related Substructural Quantities, *Mater. Sci. Eng. A-Struct. Mater. Proper. Microstruct. Process.*, 1992, **151**, p 161–168
27. F. Dobes, The Influence of Subgrain Boundary Migration on Modeling of the Response to Stress Change in Creep, *Mater. Sci. Eng. A-Struct. Mater. Proper. Microstruct. Process.*, 1993, **167**, p 31–36
28. S.L. Atkins and J.C. Gibeling, Finite Element Model of the Effects of Primary Creep in an Al-SiC Metal Matrix Composite, *Metall. Mater. Trans. A-Phys. Metall. Mater. Sci.*, 1995, **26**, p 3067–3079
29. H.H. Pan and G.J. Weng, Determination of Transient and Steady-State Creep of Metal-Matrix Composites by a Secant-Moduli Method, *Compos. Eng.*, 1993, **3**, p 661–674
30. C. Cheng and N. Aravas, Creep of Metal-Matrix Composites with Elastic Fibers .1. Continuous Aligned Fibers, *Int. J. Solids Struct.*, 1997, **34**, p 4147–4171

31. S.R. Agnew, D.W. Brown, S.C. Vogel, and T.M. Holden, In-Situ Measurement of Internal Strain Evolution During Deformation Dominated by Mechanical Twinning, *Ecrs 6: Proceedings of the 6th European Conference on Residual Stresses*, A.M. Dias, Ed., 404-4, 2002, p 747–752
32. M.M. Myshlyaev, H.J. McQueen, A. Mwembela, and E. Konopleva, Twinning, Dynamic Recovery and Recrystallization in Hot Worked Mg-Al-Zn Alloy, *Mater. Sci. Eng. A*, 2002, **337**(1-2), p 121–133
33. H.J. McQueen, M.M. Myshlyaev, and A. Mwembela, Microstructural Evolution and Strength in Hot Working of ZK60 and Other Mg Alloys, *Can. Metall. Quart.*, 2003, **42**(1), p 97–112
34. O. Sivakesavam, I.S. Rao, and Y.V.R.K. Prasad, Processing Map for Hot-Working of as Cast Magnesium, *Mater. Sci. Technol.*, 1993, **9**(9), p 805–810
35. P. Klimanek and A. Potzsch, Microstructure Evolution Under Compressive Plastic Deformation of Magnesium at Different Temperatures and Strain Rates, *Mater. Sci. Eng. A-Struct. Mater. Proper. Microstruct. Process.*, 2002, **324**(1-2), p 145–150
36. D.O. Northwood, K.E. Daly, and I.O. Smith, Work-Hardening Rates During the High Temperature Creep of Magnesium Determined from the Instantaneous Strain on Sudden Stress Changes, *Mater. Sci. Eng.*, 1985, **72**(1), p 51–63
37. S.S. Vagarali and T.G. Langdon, Deformation Mechanisms in h.c.p. Metals at Elevated Temperatures–II. Creep Behavior of a Mg-0.8% Al Solid Solution Alloy, *Acta Metall.*, 1982, **30**(6), p 1157–1170
38. M. Regev, E. Aghion, A. Rosen, and M. Bamberger, Creep Studies of Coarse-Grained AZ91D Magnesium Castings, *Mater. Sci. Eng. A*, 1998, **252**(1), p 6–16
39. X. Wu and Y. Liu, Superplasticity of Coarse-Grained Magnesium Alloy, *Scripta Mater.*, 2002, **46**, p 269–274
40. W.A. Backofen, I.R. Tumer, and D.H. Avery, *Trans ASM*, 1964, **57**, 995–985. Also see Ref 42, Chapter 5, p 80–104
41. X. Wu, H. Hao, Y. Liu, F. Zhu, J. Jiang, R. Krishnamurthy, S. Wang, P.E. Smith, W. Bland, and G.D. Pfaffmann, Elevated Temperature Formability of Some Engineering Metals for Gas Forming of Automotive Structures, *SAE J. Mater. Manuf.*, 2001, **110**(5), p 1045–1056 ((SAE Paper No. 2001-01-3103))
42. X. Wu, S. Wang, Y. Liu, and R. Krishnamurthy, Deformation and Tube Gas Bulging of AZ31B Magnesium Alloy at Elevated Temperatures Simulated by Crystal Plasticity and FEA, *Dislocations, Plasticity and Metal Forming, Proceedings of PLASTICITY 2003: The 10th Int. Symp. On Plasticity and Its Current Applications*, A. S. Khan, Ed., July 7–11, 2003, Quebec City, Canada. International Journal Plasticity, NEAT press, Maryland, p 567–569
43. Y. Liu and X. Wu, An Electron-Backscattered Diffraction Study of the Texture Evolution in a Coarse-Grained AZ31 Magnesium Alloy Deformed in Tension at Elevated Temperatures, *Metall. Mater. Trans. A-Phys. Metall. Mater. Sci.*, 2006, **37A**(1), p 7–17
44. W.F. Hosford and R.M. Caddell, *Metal Forming: Mechanics and Metallurgy.* 2nd ed., Prentice Hall, Englewood Cliffs, NJ, 1993